gree. We associate the characteristic semi-invariant factors with each combination of vertices. If one combines the semi-invariant factors with the number of ways that the single vertex may be resolved into the several vertices, and then performs a sum over the various decompositions, one will get the correct weight of unity. The equation reads

$$1=\sum_{j=1}^{n}\left[\sum_{m_1,m_2,\ldots m_j}{}' \binom{2n}{2m_1,\ 2m_2,\ \ldots,\ 2m_j}\left(\prod_{i=1}^{j} M_{2m_i}^{0}\right)\right], \tag{A1}$$

where j is the number of different vertices in the decomposition and the prime on the second sum means $\sum_{i=1}^{j} 2m_i = 2n$ for the $2m_i$ having possible values from 2 to $2n$.

The set of equations for $n=1, 2, \ldots$ will generate the values of M_2^0, $M_4^0, \ldots$. But the semi-invariant M_{2n}^0 is also the coefficient of $x^{2n-1}/(2n-1)!$ in the expansion of $\tanh x$. This identification follows from writing the expansion of $\tanh x$, integrating to produce $\ln(\cosh x)$, and then taking the exponential to produce $\cosh x$. The final step is to equate the coefficient of x^{2n} in the expansion of $\cosh x$ and in the expression resulting from the operations described in the above statement. It will be seen that the recursion relation obtained for the coefficient in the expansion of $\tanh x$ is identical to the recursion relation in Eq. (A1) of the semi-invariants.

[1]For a general review of the Ising model and the method of the high-temperature expansion, see C. Domb, Advan. Phys. 9, 149 (1960); 9, 245 (1960).

[2]M. F. Sykes, J. L. Martin, and D. L. Hunter, Proc. Phys. Soc. (London) 91, 671 (1967).

[3]For example, see G. Horowitz and H. Callen, Phys. Rev. 124, 1757 (1961); M. Coopersmith and R. Brout, *ibid.* 130, 2539 (1963); F. Englert, *ibid.* 129, 567 (1963); R. Brout, *Phase Transitions* (Benjamin, Amsterdam, 1965), pp. 33–38.

[4]The spherical model is defined by T. H. Berlin and M. Kac, Phys. Rev. 86, 821 (1952).

[5]The "generalized" spherical model is defined by J. Philhours and G. L. Hall, Phys. Rev. 177, 976 (1969).

[6]Rules (b) and (d) are given in R. Brout, *Phase Transitions* (Benjamin, Amsterdam, 1965), p. 36, as his rules (4) and (3), respectively.

[7]G. A. Baker, Jr., in *Advances in Theoretical Physics*, edited by K. A. Brueckner (Academic, New York, 1965), Vol. I.

[8]C. Domb and N. W. Dalton, Proc. Phys. Soc. (London) 89, 859 (1966).

[9]M. E. Fisher and M. F. Sykes, Physica 28, 959 (1962).

[10]N. W. Dalton and D. W. Wood, J. Math. Phys. 10, 1271 (1969).

[11]M. Lax, Phys. Rev. 97, 629 (1954).

PHYSICAL REVIEW B VOLUME 4, NUMBER 3 1 AUGUST 1971

Magnetic Excitations in Antiferromagnetic CoF_2. I. Spin-Optical-Phonon Interaction

S. J. Allen, Jr. and H. J. Guggenheim
Bell Telephone Laboratories, Murray Hill, New Jersey 07974
(Received 11 January 1971)

The interaction of the low-lying magnons and excitons with the E_g optical phonon in antiferromagnetic CoF_2 is directly observed by measuring the magnetic-dipole intensity transferred from magnetic excitations to the otherwise optically inactive E_g lattice mode. The anomalous behavior of the frequency, linewidth, and magnetic-dipole intensity of this phonon have been measured as the temperature is raised from 4.2 °K through the Néel point (37.7 °K) to $\sim 4.5T_N$ (180 °K). The frequency drops continuously with a break in slope at the Néel point, while the linewidth narrows by more than a factor of 3 when the temperature passes through the Néel point. A theory of the temperature dependence of the transferred intensity is derived which distinguishes two contributions. The first is proportional to the sublattice magnetization and vanishes in the paramagnetic state; the second is proportional to the square of the Boltzmann factor for the exciton states and vanishes only at arbitrarily high temperature. By fitting the experimental temperature dependence of the intensity to the theory, the local spin-lattice-interaction parameters for the E_g distortions can be determined.

I. INTRODUCTION

Unquenched orbital motion in the single-ion ground state of Co^{2+} significantly alters the magnetic properties of the two-sublattice antiferromagnet CoF_2. The magnetic structure[1] consists of moments parallel and antiparallel to the tetragonal axis of the rutile crystal structure and is the

same as that of the classic and thoroughly studied MnF_2. Here, however, the similarity ends. Unlike MnF_2, in which the anisotropy field, acting on the $S=\frac{5}{2}$ manifold of the Mn^{2+} ion, is much less than the exchange field, in CoF_2 the tetragonal and orthorhombic anisotropy fields acting on the $S=\frac{3}{2}$ manifold are in fact greater than the exchange fields present in the ordered state. However, the exchange field is not small compared to the splitting produced by the crystal field, and the entire $S=\frac{3}{2}$ manifold must be included in any quantitative description of the magnetic properties of CoF_2. This fact was first appreciated by Nakamura and Taketa[2] who with little experimental data qualitatively explained the anomalous temperature dependence of the susceptibility[3] of CoF_2. Similarly, the spectrum of spin-wave excitations in CoF_2 bears little resemblance to the twofold degenerate spin-wave branch which evolves from the Mn^{2+} $S=\frac{5}{2}$ manifold in MnF_2. In addition to a low-lying twofold degenerate transverse-spin-wave excitation first observed in the far infrared by Richards,[4] a high-lying twofold degenerate transverse branch, as well as a magnetic Davydov split longitudinal-spin-wave excitation can be seen. These were most clearly demonstrated by Cowley, Martel, and Stevenson[5] by neutron scattering and less clearly in some preliminary infrared studies reported by Barker and Ditzenberger.[6] Theories of the lowest spin-wave branch were constructed by Kamimura[7] and Lines[8] before data on the high-lying branches were available. Although a good fit to the lowest spin-wave branch can be obtained (using Lines's theory in particular), attempts to straightforwardly extend the theory to include the higher branches have been successful only from a qualitative point of view.[5]

It is not surprising that one cannot obtain all the spin-wave energies with only the static anisotropy field and a simple isotropic spin-spin interaction operating in the $S=\frac{3}{2}$ manifold. In addition to the large single-ion anisotropy field, the unquenched orbital motion must also produce complex multipole-multipole spin interactions as well as appreciable dynamic spin-lattice coupling. The multipole-multipole spin interactions appear as anisotropic and antisymmetric bilinear spin interactions, dipole-octupole and quadrupole spin interactions, as well as changes in the effective single-ion anisotropy. Terms of this form were first discussed by Van Vleck [9] and Stevens,[10] later by Moriya and Yosida,[11] and most recently thoroughly treated by Levy[12] and Elliot and Thorpe.[13] Birgeneau *et al.*[14] have shown them to be most important in rare-earth compounds where the higher-order spin-spin interactions are expected and are found to be as important as the lowest-order isotropic spin-spin interaction. In transition-metal compounds the higher-order terms are usually less important than the isotropic bilinear spin-spin interaction. Nevertheless, they do manifest themselves most clearly by perturbing spin arrangements, such as the weak ferromagnetism produced by the Moriya[15]-Dzialoshinski[16] antisymmetric exchange. In CoF_2, however, none of the higher-order terms perturb the simple antiparallel two-sublattice spin structure, and the importance of these terms may be only inferred from the dynamics of the spins determined from spin-wave energies, or nonlinear splitting factors of the spin-wave modes produced by applying a magnetic field perpendicular to the spin direction.

Dynamic spin-lattice coupling can be treated either by calculating an effective spin-spin coupling produced by the virtual emission and absorption of phonons or by diagonalizing the spin system and phonon system at the same time. The former approach has been used by Orbach and Tachiki,[17] Baker and Mau,[18] McMahon and Silsbee,[19] and Allen.[20,21] Such perturbative approaches fail when the spin waves and phonons are nearly degenerate. This situation is best treated by exactly diagonalizing a truncated spin-phonon Hamiltonian as described in the experiments of Hay and Torance[22] and Dolling and Cowley.[23]

Moriya[24] pointed out that large magnetoelastic effects are expected in CoF_2. Experimentally they have been observed in piezomagnetic measurements,[25] stress dependence of the antiferromagnetic resonance,[26] anomalies in the sound velocity,[27] and thermal conductivity.[28] Although all of these measurements indicate that magnetoelastic effects are important, none have been used to deduce either the microscopic spin-lattice interaction or to describe how such a coupling alters the spin-wave spectra.

A good description of the observed spin-wave spectra at $T=0\,^{\circ}K$ could be obtained by including all possible terms that describe the effects of multipole-multipole spin interactions and the spin-phonon coupling. However, the parameters extracted from such a fit would be ambiguous because the off-diagonal exchange and the spin-phonon coupling often lead to spin-interaction terms that have the same phenomenological form. The object of these two papers is to present a quantitative picture of the spectrum of spin-wave excitations that arise from the $S=\frac{3}{2}$ single-ion manifold in CoF_2. The aforementioned ambiguity is partially relieved by independently determining two of the spin-phonon interaction parameters by observing the magnetic-dipole intensity transferred from the spin system to the E_g optical phonon by the spin-lattice interaction.[29] We also present far-infrared absorption data which extend the initial work of Richards[4,26] and Barker *et al.*[6] to include all the $k=0$ excitations of the spin system. Important in

the analysis is the magnetic field dependence of these modes both for fields parallel as well as perpendicular to the spin direction. In the final analysis, the experimentally determined spin-lattice coupling, the anisotropy fields and g factors determined from the diamagnetic isomorph MgF_2 and a simple isotropic exchange produce a quantitative fit to the $k=0$ excitation energies and wave functions. The detailed influence of multipole spin interactions is left unresolved, but the good agreement achieved without invoking such terms suggests that they are less important than one would have anticipated.

The two papers are divided in the following manner. In the first we discuss the transfer of magnetic-dipole intensity to the otherwise optically inactive E_g phonon. This experiment and its analysis is rather crucial for it unambiguously determines the magnitude of two of the stronger spin-phonon coupling parameters. Since the details of the spin excitations are less important in this paper, they are treated in the simplest approximation—molecular field theory. A detailed analysis of the temperature dependence allows us to extract a set of local spin-phonon coupling parameters. The perturbation calculation performed in this paper is different from that published previously.[29] It is, however, an improvement on the earlier calculation because it contains the temperature dependence of various matrix elements and is physically more transparent. A recent calculation of this effect by Mills and Ushioda[30] provides some interesting ideas with regard to the linewidth of the E_g phonon which are discussed later, but is too phenomenological to help extract the microscopic spin-phonon coupling that is required in the second paper.

With the spin-phonon coupling in hand, we proceed in the second paper to examine in detail the spectrum of spin-wave excitations at $k=0$. The single-ion anisotropy field is taken from the diamagnetic isomorph MgF_2 while the exchange constant is taken from those spin-wave modes that do not appear to interact strongly with phonons. The energies and wave functions obtained in the second paper appear to agree well with the far-infrared absorption experiments and provide a quantitative description of the spin excitations in the system.

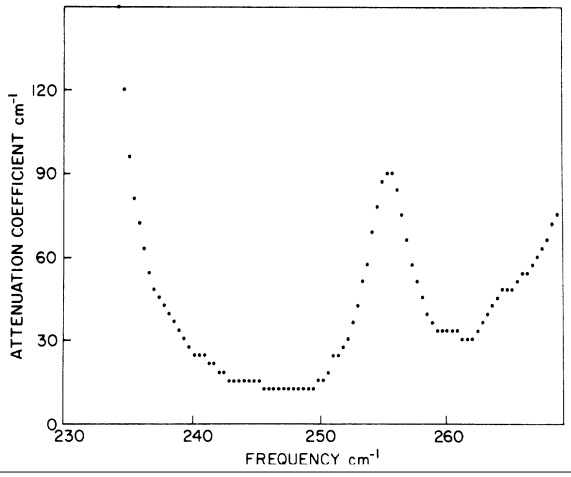

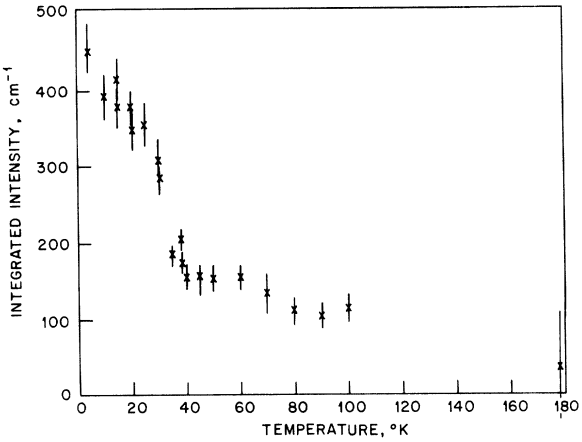

FIG. 2. Integrated magnetic-dipole intensity versus temperature (Ref. 28).

The remainder of this paper proceeds as follows. In Sec. II we describe the experimental observation of the spin coupling to the E_g phonon in CoF_2. Section III develops the theory of the temperature dependence of the transferred magnetic-dipole intensity while in Sec. IV the theory is used to deduce the microscopic spin coupling parameters. Section V is reserved for discussion of the assumptions and approximations used in the analysis as well as consideration of the order of magnitude of the observed parameters.

II. EXPERIMENT

The far-infrared absorption measurements were performed on thin, ~0.2 mm, oriented plates of CoF_2 cut from a single-crystal boule grown by the Bridgman technique. Additional experiments were performed on a single crystal kindly provided by Martel of the Chalk River Laboratories. Absorption spectra were taken with a Michelson Fourier transform spectrometer,[31] while temperature measurement and control were obtained with a forward-biased GaAs diode thermometer in conjunction with a heater and feedback control circuit. Temperature stability and accuracy to better than

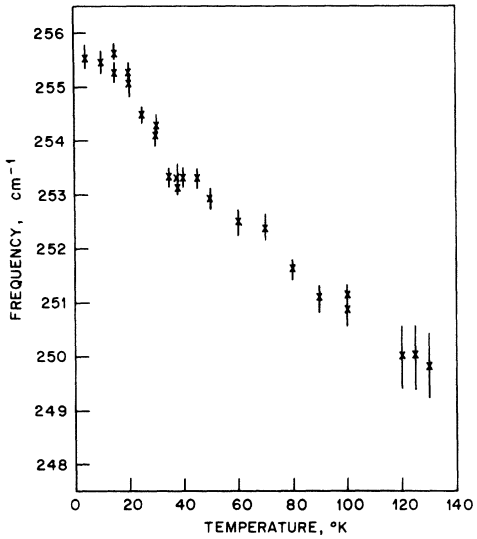

FIG. 3. Resonant frequency versus temperature.

the c axis at 256 cm^{-1} at 4.2 °K (Fig. 1). As the temperature is raised to the Néel point, the integrated intensity falls rapidly to roughly $\frac{1}{3}$ the low-temperature value (Fig. 2), where intensity and frequency are expressed in wave-number units. Proceeding to temperatures as high as $4.5kT_N \approx 180$ °K, the intensity continues to fall but less dramatically. Good measurements of the integrated intensity cannot be obtained above ~180 °K due to the large linebreadth. The frequency of the mode changes in a similar but less striking way. From 4.2 to 130 °K the line position shifts downward by approximately 6 cm^{-1}. There is a slight break at the Néel point (Fig. 3).

The behavior of the linewidth as a function of temperature is shown in Fig. 4. Simple electronic excitations in ordered magnetic systems usually broaden as the system approaches the spin-disordering temperature. Likewise, phonon absorptions usually show a monotonic increase in linewidth with temperature. The absorption line in question, however, narrows by more than a factor of 3 when the temperature is raised from 4.2 °K to $T_N = 37.7$ °K. This line narrowing is perhaps one of the most peculiar results of these experiments and has been observed by Raman scattering from the A_{1g} mode.[32] The theory that is developed in the remainder of this paper includes no line broadening and consequently cannot explain the observation.[30]

The mode is interpreted as the $k = 0$, normally infrared inactive, E_g optical phonon for the following reasons. First the frequency of the excitation agrees with current measurements of the E_g energy. An estimate of the low-temperature E_g energy can be had by examining the Raman experiments of Porto, Fleury, and Damen[33] on MnF_2 and FeF_2, the neutron experiments of Martel, Cowley, and Stevenson[5] on CoF_2, or Raman experiments on CoF_2 by MacFarlane and Ushioda.[33] Extrapolating from the E_g modes of MnF_2 and FeF_2 gives a value of ~265 cm^{-1} for the E_g mode, ~10 cm^{-1} too high. The published neutron data are not very useful for it does not appear that enough modes were resolved above 200 cm^{-1}. Nevertheless, there are $k = 0$ phonon modes in the vicinity of 250 cm^{-1}. MacFarlane and Ushioda[33] measure directly the E_g mode in CoF_2 to be 245 cm^{-1} at room temperature and ~256 cm^{-1} at low temperature. Clearly these data must be weighed most heavily in the assignment. The discrepancy of 10 cm^{-1} between their room-temperature data and the present 4.2 °K infrared absorption data agrees, perhaps fortuitously, with the shift predicted by the spin-phonon coupling discussed in the second of these papers. Since the spin system is saturated at high temperatures the perturbation of the phonon by the spins vanishes. At low temperatures, however, the frequency is expected to be shifted by the full perturbation, ~10 cm^{-1}. Second pure electronic excitations are excluded by the peculiar linewidth behavior discussed above and the relatively weak temperature dependence of the frequency. Electronic impurity excitations are excluded since impurity concentrations of the order of 15–20% would be necessary to obtain the observed magnetic-dipole intensity. It should be noted that the group theory for CoF_2 allows the E_g phonons as a magnetic-dipole transition. The evidence suggests that we interpret this absorption as the $k = 0$, E_g phonon allowed as a transverse magnetic-dipole absorption by coupling with the spins on the Co^{2+} ions. Further weight to this assignment fol-

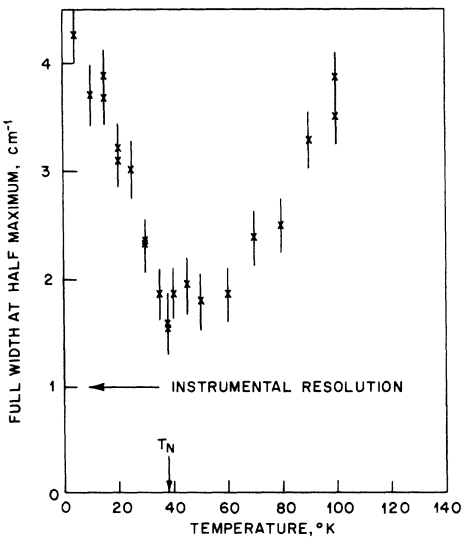

FIG. 4. Full width at half-maximum versus temperature (Ref. 28).

lows from the fact that this interpretation leads to the proper temperature dependence of the transferred intensity as well as a quantitative description of the spin excitations.

III. THEORY

The discussion of the theory of the coupling between the $k=0$, E_g phonons and the spin-wave excitations proceeds in the following manner. We first briefly review the Co^{2+} ion in CoF_2 and the diamagnetic isomorph MgF_2. It is assumed that the properties of the Co^{2+} ion from ~4.2 °K to ~200 °K can be described accurately by the lowest four levels. That is, all the interactions either between the Co^{2+} ions and the lattice or between the Co^{2+} ion and other Co^{2+} ions can be described in terms of suitable operators in this fourfold effective $S=\frac{3}{2}$ manifold. This approach has been successfully used by Lines[8] to obtain the lowest spin-wave excitations in CoF_2. One then proceeds by turning on both the spin-spin interactions and the spin-phonon interactions. Since the present discussion focuses on the spin-phonon coupling and its effect on the phonons, the spin-spin interactions are treated in the simplest approximation—the mean-field approximation. Although symmetry considerations allow many terms in the spin-phonon Hamiltonian, we keep only that term which gives coupling to the E_g phonon. First-order perturbation theory enables us to find the mixing of the phonon and spin excitations. Using the mean-field approximation to specify the spin state as a function of temperature we arrive finally at the temperature dependence of the magnetic-dipole intensity transferred to the E_g phonons.

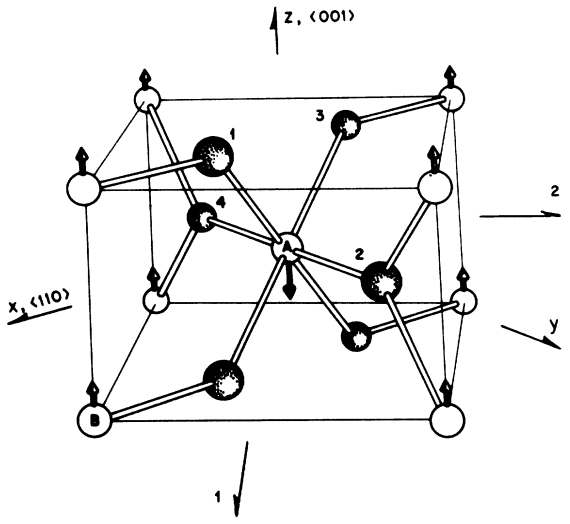

FIG. 5. CoF_2 crystal structure showing magnetic ordering below 37.7 °K (Ref. 1).

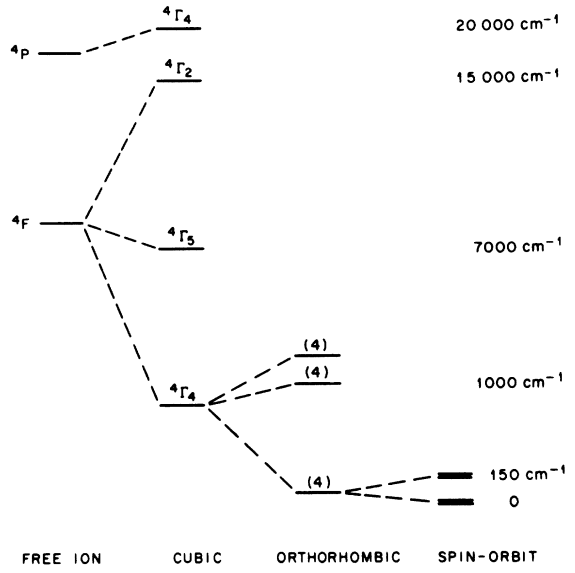

FIG. 6. Crystal-field splitting of the d^7 manifold by the orthorhombic crystal field (Ref. 31).

A. Single-Ion Hamiltonian

CoF_2 crystallizes in the rutile structure shown in Fig. 5. An orthorhombically distorted octahedron of F^- ions surrounds each Co^{2+} site. The Co^{2+} sites on the corners of the unit cell (B sites) experience the same crystal-field interaction as the site at the center (A site) but rotated through 90°. Below 37.7 °K the spin at the body center of the unit cell (A sites) aligns along the c axis antiparallel to the spins on the corner sites, thus forming a simple two-sublattice antiferromagnet.[1]

Three holes in the d shell of the free Co^{2+} ion couple to give a quartet F state separated by ~ 20 000 cm^{-1} from the next highest state in the d^7 configuration a quartet P.[34] These levels are shown schematically in Fig. 6. The cubic component of the crystal field provided by the six fluorines splits the orbital degeneracy of the F state and also mixes the lowest component, a $^4\Gamma_4$, with the ^4P which transforms like a $^4\Gamma_4$. The orthorhombic component of the crystal field further lifts the orbital degeneracy of the orbital triplet Γ_4 into three orbitally nondegenerate levels. The orbital ground state is separated by approximately 800 and 1000 cm^{-1} from the next two excited orbital states (labeled E_1 and E_2). Finally we turn on the spin-orbit coupling which lifts the fourfold spin degeneracy associated with each of these orbital states leaving six Kramers doublets. The pair of Kramers doublets evolved from the ground state are separated by only ~150 cm^{-1} whereas the four excited doublets are removed by ~1000 cm^{-1} from the ground state. For

temperatures less than room temperature only the lowest pair of doublets need be considered in describing the magnetic state of the system.

Since the spin-orbit matrix elements ($\lambda \approx 230$ cm^{-1}) are not small compared to E_1 and E_2 (~ 1000 cm^{-1}), appreciable orbital motion is coupled to the $S=\frac{3}{2}$ ground state. Fortunately, since λ/E_1 and λ/E_2 are less than unity, perturbation theory can be used to treat the mixing between the lowest pair of doublets and the states E_1 and E_2. An effective spin Hamiltonian can be constructed but higher-order terms are expected to be important. For instance, to obtain accurate values ($\approx 10\%$ accuracy) for the crystal-field energies for the lowest pair of doublets, perturbations to third order are necessary.

The orthorhombic crystal-field Hamiltonian for the lowest two doublets, an $S=\frac{3}{2}$ manifold, is given by the following[8]:

$$-\delta S_z^2+\gamma(S_x^2-S_y^2)\ . \tag{1}$$

This is, of course, the most general form that can be obtained for the $S=\frac{3}{2}$ manifold. Higher powers of $\vec{S}$ can be reduced to second-order terms of the form (1) if we remain in the $S=\frac{3}{2}$ manifold. A magnetic field applied to the system adds terms of the form $g_xH_xS_x+g_yH_yS_y+g_zH_zS_z$. This is not complete, however, for we should also include terms third order in $\vec{S}$ such as $S_z^3H_z$. These terms, however, will be of the order of λ^3/E^3 (0.03) of the first-order terms and are neglected.

The two sets of Kramers doublets given by (1) are separated by

$$\epsilon_0=2(\delta^2+3\gamma^2)^{1/2}\ . \tag{2}$$

The wave functions generated are the following:

$$\begin{aligned}|3,4\rangle&=b\left|\pm\tfrac{3}{2}\right\rangle-a\left|\mp\tfrac{1}{2}\right\rangle\ ,\\ |1,2\rangle&=a\left|\pm\tfrac{3}{2}\right\rangle+b\left|\mp\tfrac{1}{2}\right\rangle\ ,\end{aligned} \tag{3}$$

where the first wave-function index goes with the upper sign and

$$a=\left(\frac{\frac{1}{2}\epsilon_0+\delta}{\epsilon_0}\right)^{1/2},\quad b=-\left(\frac{\frac{1}{2}\epsilon_0-\delta}{\epsilon_0}\right)^{1/2}. \tag{4}$$

If Eq. (1) describes the Co^{2+} ions on the A sites, the body center in Fig. 5, then we obtain the result for the B sites, corner sites in Fig. 1, by changing the sign of γ in (1) and the sign of b in (3).

B. Exchange Interactions

The exchange interactions between Co^{2+} ions are treated in this paper with two simplifying approximations. First we assume that the interaction between spins, each in the $S=\frac{3}{2}$ manifold, can be described by a single isotropic exchange term, $J\vec{S}_1\cdot\vec{S}_2$. Higher-order terms leading to both anisotropic bilinear exchange as well as terms of the form quadrupole quadrupole and dipole octupole theoretically appear as $(\lambda^2/E^2)J$ ($\approx\frac{1}{10}J$). The following paper and the lack of dispersion of the spin waves on the zone boundary[5] indicate that these higher-order terms are at least a factor of 3 smaller than this estimate and are neglected. Second, mean-field theory is used to describe the spin excitations above and below T_N. This is not as bad an approximation as it would first appear for the following reason. The E_g phonon interacts primarily with the upper transverse-spin-wave branch (labeled AD in the papers by Martel *et al.*[5]), which is nearly flat throughout the Brillouin zone both above and below T_N. Theoretically this is expected. Furthermore apart from the spin-phonon interactions the energy of this excitation equals the mean-field splitting to within $\sim 1\%$.

Within the framework of these assumptions one complication must be included. As was first suggested by Lines, mixing of the excited Kramers doublet into the ground doublet by the molecular field must be included to obtain quantitative results. This produces a nonlinear splitting of the levels of this manifold as well as a modification of the wave functions in (3) as the system orders magnetically. In this discussion we include only first-order changes in wave functions and matrix elements. This approximation is good to within 10%.

We then diagonalize the following spin Hamiltonian correct to first order in the molecular field, $\alpha=zJ\langle S_z\rangle$:

$$-\delta S_z^2\pm\gamma(S_x^2-S_y^2)\mp\alpha S_z\ , \tag{5}$$

where the upper sign refers to the A sites and the lower sign to the B sites. The resulting energies and wave functions[8] for the body-centered site are

$$\begin{aligned}E_4&=\tfrac{1}{2}\alpha+\tfrac{1}{2}\epsilon_0-(2\delta/\epsilon_0)\alpha+(\alpha^2/\epsilon_0)(1-4\delta^2/\epsilon_0^2)\ ,\\ E_3&=\tfrac{1}{2}\alpha+\tfrac{1}{2}\epsilon_0+(2\delta/\epsilon_0)\alpha+(\alpha^2/\epsilon_0)(1-4\delta^2/\epsilon_0^2)\ ,\\ E_2&=\tfrac{1}{2}\alpha-\tfrac{1}{2}\epsilon_0+(2\delta/\epsilon_0)\alpha-(\alpha^2/\epsilon_0)(1-4\delta^2/\epsilon_0^2)\ ,\\ E_1&=\tfrac{1}{2}\alpha-\tfrac{1}{2}\epsilon_0-(2\delta/\epsilon_0)\alpha-(\alpha^2/\epsilon_0)(1-4\delta^2/\epsilon_0^2)\end{aligned} \tag{6}$$

and

$$\begin{aligned}|4\rangle&=d'\left|-\tfrac{3}{2}\right\rangle-c'\left|\tfrac{1}{2}\right\rangle\ ,\\ |3\rangle&=b'\left|\tfrac{3}{2}\right\rangle-a'\left|-\tfrac{1}{2}\right\rangle\ ,\\ |2\rangle&=c'\left|-\tfrac{3}{2}\right\rangle+d'\left|\tfrac{1}{2}\right\rangle\ ,\\ |1\rangle&=a'\left|\tfrac{3}{2}\right\rangle+b'\left|-\tfrac{1}{2}\right\rangle\ ,\end{aligned} \tag{7}$$

where

$$a' = a + 2ab^2\alpha/\epsilon_0 ,$$

$$b' = b - 2a^2b\alpha/\epsilon_0 ,$$

$$c' = a - 2ab^2\alpha/\epsilon_0 , \qquad (8)$$

$$d' = b + 2a^2b\alpha/\epsilon_0 .$$

Again for the corner sites $b' \rightarrow -b'$ and $d' \rightarrow -d'$.

C. Spin-Phonon Interactions

At $k = 0$ the two degenerate phonon normal modes that transform like E_g are shown in Fig. 7.[35] They appear at the Co^{2+} site as a shear deformation of the crystal field, transforming as zx or zy. It is clear that the shear deformation shown in Fig. 7(a) interacts with the A sites differently than it interacts with the B sites. Consequently we need two constants to describe the interaction between a local shear distortion and the two Co^{2+} sites A and B. However, the interaction of the local (zy) shear deformation with the A and B sites can be obtained from the (zx) interaction by rotating the crystal through 90° and translating A into B. Further, if we assume that the only important local spin-phonon coupling is produced by the above-mentioned shear distortions we need only two parameters to describe the interaction. The spin-phonon coupling Hamiltonian that is obtained is the following:

$$\frac{1}{N^{1/2}} \sum_i \sum_{\vec{k}} \sum_p X_{\vec{k},p}\, e^{-j\vec{k}\cdot\vec{r}_i} \{[\eta Q^A_{zx}(i) f^{1,3}_{\vec{k},p} + \xi Q^B_{zx}(i) g^{1,3}_{\vec{k},p}] + [\eta Q^B_{zy}(i) f^{2,4}_{\vec{k},p} + \xi Q^A_{zy}(i) g^{2,4}_{\vec{k},p}]\} . \qquad (9)$$

In Eq. (9) i runs over the N unit cells, $\vec{k}$ is the phonon wave vector and p is the branch index for the phonon. $X_{\vec{k},p}$ is the normal coordinate displacement for $\vec{k}$, p phonon. [In second-quantized form this would become $j(\alpha_{\vec{k},p} - \alpha^*_{-\vec{k},p})(\hbar/2m\omega_{\vec{k},p})^{1/2}$, where $e^{-j\vec{k}\cdot\vec{r}_i}$ is the phase factor for the phonon of wave vector $\vec{k}$ in the ith unit cell.] $Q^A_{zx}(i)$ is the quadrupole spin operator in the ith unit cell at the A site transforming like zx

$$Q_{zx} = \tfrac{1}{2}(S^zS^x + S^xS^z) . \qquad (10)$$

The functions f and g are the projections of the $\vec{k}$, p normal mode on the local shear distortions shown in Fig. 7. In Ziman's[36] notation for the phonon eigenvectors $e^{\alpha}_{\vec{k},r,p}$ we have

$$f^{1,3}_{\vec{k},p} = (1/2\sqrt{2})(-e^{x\,*}_{\vec{k},1,p} + e^{x\,*}_{\vec{k},3,p})(1 + e^{+jk_zc}) ,$$

$$g^{1,3}_{\vec{k},p} = (1/\sqrt{2})(-e^{x\,*}_{\vec{k},1,p} + e^{x\,*}_{\vec{k},3,p}\, e^{j(k_1a - k_2a)})\, e^{+jk_zc} ,$$

$$g^{2,4}_{\vec{k},p} = (1/\sqrt{2})(e^{x\,*}_{\vec{k},2,p} - e^{x\,*}_{\vec{k},4,p}) , \qquad (11)$$

$$f^{2,4}_{\vec{k},p} = (1/2\sqrt{2})(e^{x\,*}_{\vec{k},2,p}\, e^{+jk_za} - e^{x\,*}_{\vec{k},4,p}\, e^{-jk_1a})(1 + e^{+jk_zc}) .$$

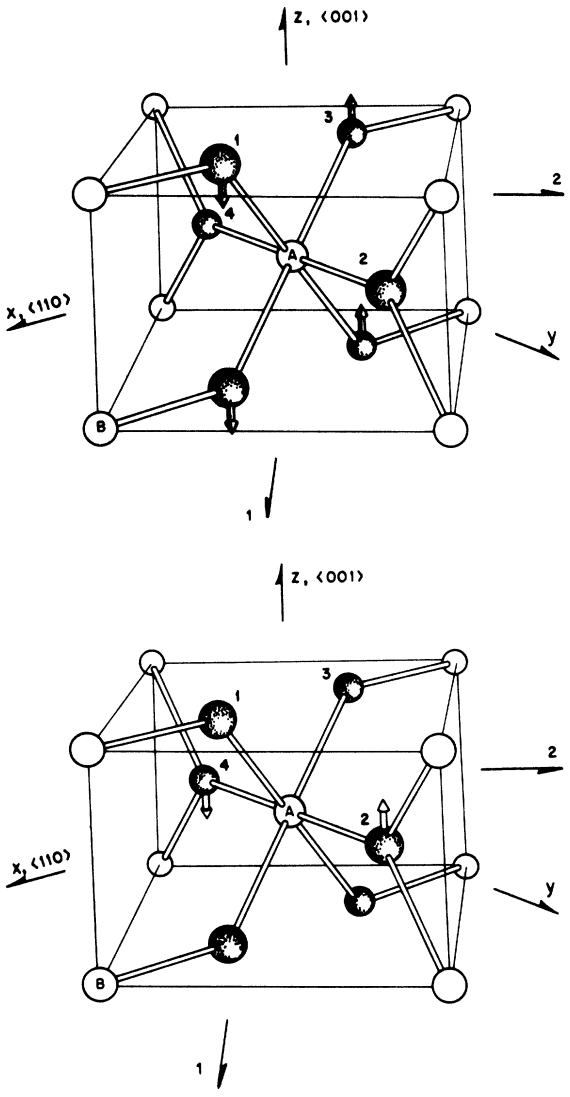

FIG. 7. Displacements about the A site produced by the two E_g normal modes.

Since we only use results at $k = 0$, we need only recognize that f and $g = 0$ at $k = 0$ except for $f^{1,3}_{\vec{k}=0,p=E_g,zx}$, $g^{1,3}_{\vec{k}=0,p=E_g,zx}$, $f^{2,4}_{\vec{k}=0,p=E_g,zy}$, and $g^{2,4}_{\vec{k}=0,p=E_g,zy}$, which are unity. η and ξ are the independent coupling parameters determining the strength of the interaction.

As previously stated, Eq. (9) assumes that only the local shear distortions of the orthorhombic crystal field which transform like zx and zy are important in the spin-phonon coupling. If we restrict our discussion to first-order mixing of spin excitations with the E_g modes, Eq. (9) is a sufficient description of the interaction. Since we contact experiment only at the $k = 0$, E_g phonons we satisfy ourselves, for the present, with this Hamiltonian.

D. Diagonalizing the Spin-Phonon Interaction

We now determine the new phonon normal modes of the system correct to first order in the spin-phonon interaction assuming that the spin excitations at some arbitrary temperature are given by a random distribution of Co^{2+} ions in the molecular field states (6, 7, 8). [For $T > T_N$ there is no molecular field and (7) reduces to (3).] Specifically we ask the following question. If we propagate a normal mode of the lattice, represented by $X_{\vec{k},\rho}\, e^{i\omega t}$, what is the magnitude and character of the accompanying spin polarization? This is solved by treating the applied distortion $X_{\vec{k},\rho}\, e^{i\omega t}$ by time-dependent perturbation theory, Hamiltonian (9) being the perturbing Hamiltonian and the molecular field Hamiltonian (5) the unperturbed part.

The results contain the following qualitative features. The local spin polarization produced by the distortion contains two terms—the first is independent of the spin orientation at the Co^{2+} site, the second depends on the spin orientation. Whereas the former always produces a spin polarization with a $\vec{k}$ vector equal to that of the lattice distortion, the latter produces a spin polarization that contains all wave vectors when there is any degree of disorder in the spins. In the latter a finite fraction of the spin polarization produced by the lattice deformation will be at the same wave vector, $\vec{k}$, as the deformation, only if there is long-range order in the spin system.

We first derive the results in the paramagnetic state $T > T_N$, then extrapolate into the ordered state. For an arbitrary temperature, T, the state of a Co^{2+} ion on the A site in the ith unit cell will be a random linear combination of the four states enumerated in Eqs. (3):

$$|\, i,\ A\,\rangle = a_1 |\,1\,\rangle + a_2 |\,2\,\rangle + a_3 e^{j\omega_0 t} |\,3\,\rangle + a_4 e^{j\omega_0 t} |\,4\,\rangle\,, \tag{12}$$

where

$$\hbar\omega_0 = \epsilon_0\,.$$

We apply the following time-dependent perturbation to the state $|\, i,\ A\,\rangle$:

$$\frac{1}{N^{1/2}}\, X_{\vec{k},\rho}\, e^{j\omega_{\vec{k},\rho} t}\, e^{-j\vec{k}\cdot\vec{r}_i} \left[\eta Q^A_{zx}(i) f^{1,3}_{\vec{k},\rho} + \xi Q^A_{xy}(i) g^{2,4}_{\vec{k},\rho}\right]. \tag{13}$$

To find the new time varying state to first order we require the matrix elements of Q_{zx} and Q_{xy} in the representation (3):

$$Q_{zx} = \begin{Vmatrix} 0 & 0 & 0 & -\frac{1}{2}\sqrt{3} \\ 0 & 0 & +\frac{1}{2}\sqrt{3} & 0 \\ 0 & +\frac{1}{2}\sqrt{3} & 0 & 0 \\ -\frac{1}{2}\sqrt{3} & 0 & 0 & 0 \end{Vmatrix}, \tag{14}$$

$$Q_{xy} = j \begin{Vmatrix} 0 & 0 & 0 & +\frac{1}{2}\sqrt{3} \\ 0 & 0 & +\frac{1}{2}\sqrt{3} & 0 \\ 0 & -\frac{1}{2}\sqrt{3} & 0 & 0 \\ -\frac{1}{2}\sqrt{3} & 0 & 0 & 0 \end{Vmatrix}. \tag{15}$$

The resulting spin polarization is found from the spin matrices in the representation (3):

$$S^x = \begin{Vmatrix} 0 & B & 0 & A \\ B & 0 & A & 0 \\ 0 & A & 0 & 1-B \\ A & 0 & 1-B & 0 \end{Vmatrix}, \tag{16}$$

where

$$A = -\tfrac{1}{2}\sqrt{3}\,(a^2 - b^2) - ab\,,$$

$$B = \sqrt{3}\,ab + b^2\,,$$

$$S^y = i \begin{Vmatrix} 0 & -D & 0 & C \\ D & 0 & -C & 0 \\ 0 & C & 0 & -(1-D) \\ -C & 0 & (1-D) & 0 \end{Vmatrix}, \tag{17}$$

where

$$C = \tfrac{1}{2}\sqrt{3}\,(a^2 - b^2) - ab\,,$$

$$D = \sqrt{3}\,ab - b^2\,,$$

and

$$S^z = \begin{Vmatrix} F & 0 & E & 0 \\ 0 & -F & 0 & -E \\ E & 0 & 1-F & 0 \\ 0 & -E & 0 & 1-F \end{Vmatrix}, \tag{18}$$

where

$$E = 2ab\,,$$

$$F = \tfrac{3}{2}a^2 - \tfrac{1}{2}b^2\,.$$

We obtain for the spin-polarization amplitude at the A site in the ith unit cell the following:

$$\delta S^A_x = X_{\vec{k},\rho}\, e^{-j\vec{k}\cdot\vec{r}_i}\, \frac{2A}{N^{1/2}}\, \frac{(\sqrt{3}/2)}{\hbar(\omega_{\vec{k},\rho}^{\,2} - \omega_0^{\,2})} \times \left[\eta f^{1,3}_{\vec{k},\rho}\, \omega_0 R^A_x(i) - j\xi g^{2,4}_{\vec{k},\rho}\, \omega_{\vec{k},\rho} I^A(i)\right], \tag{19}$$

$$\delta S^A_y(i) = X_{\vec{k},\rho}\, e^{-j\vec{k}\cdot\vec{r}_i}\, \frac{2C}{N^{1/2}}\, \frac{(\sqrt{3}/2)}{\hbar(\omega_{\vec{k},\rho}^{\,2} - \omega_0^{\,2})}$$

$$\times[-j\eta f^{1,3}_{\vec{k},p}\omega_{\vec{k},p} I^A(i) - \xi g^{2,4}_{\vec{k},p}\omega_0 R^A_x(i)]\,, \quad (20)$$

$$\delta S^A_x(i) = X_{\vec{k},p}\, e^{-j\vec{k}\cdot\vec{r}_i}\,\frac{2E}{N^{1/2}}\,\frac{(\sqrt{3}/2)}{\hbar(\omega^2_{\vec{k},p}-\omega_0^2)}$$

$$\times[-\eta f^{1,3}_{\vec{k},p}\omega_0 R^A_x(i) + \xi g^{2,4}_{\vec{k},p}\omega_0 R^A_y(i)]\,, \quad (21)$$

where $I^A(i)$ is the value of the operator

$$I = \begin{Bmatrix} +1 & & & \\ & +1 & & \\ & & -1 & \\ & & & -1 \end{Bmatrix} \quad (22)$$

at the site A in the ith cell, and

$$R^A_x(i) = \tfrac{7}{3}S^A_x(i) - \tfrac{4}{3}S^A_x(i)^3\,. \quad (23)$$

R^A_x and R^A_y are given by a similar expression in x and y. The results for the B site in the ith unit cell are obtained from (19)–(21) by

$$\eta f^{1,3}_{\vec{k},p} - \xi g^{1,3}_{\vec{k},p}\,,\quad \xi g^{2,4}_{\vec{k},p} - \eta f^{2,4}_{\vec{k},p}\,,$$

$$A \rightarrow -C\,,\quad C \rightarrow -A\,,\quad E \rightarrow -E\,. \quad (24)$$

In order to calculate the magnetic-dipole intensity for the $\vec{k}$, p phonon for an infrared magnetic field polarized transverse to c axis, we first compute the amplitude of the uniform transverse magnetization for the entire crystal carried by one $\vec{k}$, p phonon

$$\delta M_x = \sum_i \left(\frac{\delta S^A_x(i)\, g_x\,\mu_B + \delta S^B_x(i)\, g_y\,\mu_B}{X_{\vec{k},p}}\right)\left(\frac{\hbar}{2m\omega_{\vec{k},p}}\right)^{1/2}. \quad (25)$$

The square of the magnetic-dipole matrix element per unit cell is

$$\frac{|\delta M_x|^2}{N} = \frac{1}{N}\left(\frac{\hbar}{2m\omega_{\vec{k},p}}\right)\left|\sum_i \frac{\delta S^A_x(i)\, g_x\,\mu_B + \delta S^B_x(i)\, g_y\,\mu_B}{X_{\vec{k},p}}\right|^2, \quad (26)$$

which can be reduced to the following by using (19) as well as the prescription (24):

$$\frac{|\delta M_x|^2}{N} = \left(\frac{\hbar}{2m\omega_{\vec{k},p}}\right)\frac{3\mu_B{}^2}{\hbar^2(\omega_{kp}{}^2-\omega_0{}^2)^2}$$

$$\times\Big(\omega_0{}^2\,\frac{1}{N}\sum_i e^{j\vec{k}\cdot\vec{r}_i}[Ag_x\eta f^{1,3}_{\vec{k},p}R^A(0) - Cg_y\xi g^{1,3}_{\vec{k},p}R^B_x(0)]$$

$$\times[Ag_x\eta f^{1,3*}_{\vec{k},p}R^A_x(i) - Cg_y\xi g^{1,3*}_{\vec{k},p}R^B_x(i)]$$

$$+\omega^2_{\vec{k},p}\,\frac{1}{N}\sum_i e^{j\vec{k}\cdot\vec{r}_i}[Ag_x\xi g^{2,4}_{\vec{k},p}I^A(0) - Cg_y\eta f^{2,4}_{\vec{k},p}I^B(0)]$$

$$\times[Ag_x\xi g^{2,4*}_{\vec{k},p}I^A(i) - Cg_y\eta f^{2,4*}_{\vec{k},p}I^B(i)]\Big). \quad (27)$$

According to (27) the magnetic-dipole absorption of a $k=0$, infrared photon, by a phonon of arbitrary wave vector $\vec{k}$ on branch p is proportional to two sets of correlation functions evaluated at $\vec{k}$. The first, represented by the first sum in (27), has the appearance of a longitudinal spin-spin correlation function. Indeed, at low temperature when the excited doublet is not populated

$$R^A_x(i) = -M^A_x(i)/Fg\mu_B\,, \quad (28)$$

where $M^A_x(i)$ is the magnetic moment on the A site in the ith cell and $Fg\mu_B$ is its maximum possible value in the paramagnetic state. Further it is clear that the first term can give a finite fraction of the magnetic-dipole intensity to a $\vec{k}=0$ phonon only if there is a singularity in the correlation function at $\vec{k}=0$. This occurs only if there are infinite-range correlations in the longitudinal spin component, i.e., at $T<T_N$. The second term has the same properties with regard to the operator $I(i)$. Unlike the spin operator, however, there exists an infinite-range correlation for I at all temperatures. In particular,

$$\langle I(0)\, I(\infty)\rangle = \tanh^2(\hbar\omega_0/2kT)\,, \quad (29)$$

which is the square of the Boltzmann factor for the four states on each site.

The uniform magnetic-dipole absorption associated with phonons, other than the $\vec{k}=0$, $p=E_g$ phonons, will be spread over all the possible phonon frequencies and consequently experimentally undetectable. The strong absorption, found at $\vec{k}=0$, $p=E_g$, caused by the $\vec{k}=0$ singularities in the correlation functions of (27) reduces to the following:

$$\frac{|\delta M_x|^2}{N} = \left(\frac{\hbar}{2m\omega_p}\right)\frac{3\mu_B{}^2}{\hbar^2(\omega_p{}^2-\omega_0{}^2)^2}$$

$$\times\omega_0{}^2\left(\frac{M(T)}{M(0)}\right)^2(Ag_x\eta + Cg_y\xi)^2$$

$$+\omega_p{}^2\tanh^2\frac{\hbar\omega_0}{2kT}\,(Ag_x\xi - Cg_y\eta)^2\,, \quad (30)$$

where ω_p is the E_g phonon frequency and we take advantage of the fact that the first term in (27) contributes to (30) only when (28) holds. $M(T)$ is the sublattice magnetization. We make contact with the Green's-function calculation used in the previous account by noting that in Eq. (4) of Ref. 29

$$gS_x = Ag_x\,,\quad gS_y = Cg_y\,,$$

$$\beta_1 = \tfrac{1}{2}\eta\,,\quad \beta_2 = \tfrac{1}{2}\xi\,. \quad (31)$$

By examining (21), it is clear that the selection rules exclude a magnetic-dipole absorption parallel to the c axis for $\vec{k}=0$, $p=E_g$, for this would require long-range order in the transverse spin components

which exists at no temperature in CoF_2. This result is also required by group theory.

It remains to extrapolate (30) to temperatures below T_N. Below T_N, ω_0 rises rapidly and consequently the resonant term $(\omega_0^2-\omega_p^2)^{-2}$ in (30) changes substantially. We replace the fixed ω_0 in (30) with $\omega_0(T)$ measured either by neutron scattering or by far-infrared absorption.

Secondly, the matrix elements A and C change as the molecular field is applied. Specifically

$$\begin{aligned} A &= -(\sqrt{3}/2)(a'c'-b'd')-b'c' , \\ C &= (\sqrt{3}/2)(a'c'-b'd')-b'c' , \end{aligned} \tag{32}$$

and substituting from (8) we have, keeping only terms first order in the molecular field $\alpha(T)$:

$$\begin{aligned} A(T) &= A(\infty)+2ab\,\alpha(T)/\epsilon_0 , \\ C(T) &= C(\infty)+2ab\,\alpha(T)/\epsilon_0 . \end{aligned} \tag{33}$$

The quadrupole matrix elements between the doublets have only second-order changes due to α. The new quadrupole matrix elements that appear between the states of the lowest doublet are ignored since the lowest spin-wave excitations are too far from the E_g phonon to transfer appreciable intensity.

To extrapolate below T_N, we use the following:

$$\begin{aligned} \frac{|\delta M_x|^2}{N} &= \frac{\hbar}{2m\omega_p}\,\frac{3\mu_B^2}{\hbar^2[\omega_p^2-\omega_0(T)^2]^2} \\ &\times\omega_0^2\left[\frac{M(T)}{M(0)}\right]^2[A(T)g_x\eta+C(T)g_y\xi]^2 \\ &+\omega_p^2\tanh^2\frac{\hbar\omega_0(T)}{2kT}\,[A(T)g_x\xi-C(T)g_y\eta]^2 . \end{aligned} \tag{34}$$

The measured integrated intensity is proportional to $|\delta M_x|^2/N$ and is given as follows:

$$\int\alpha\,d\nu=\frac{2\pi^2 n\mu_0\rho\nu_p}{hc}\,\frac{|\delta M_x|^2}{N}\ \mathrm{cm}^{-2} , \tag{35}$$

where n is the index of refraction, μ_0 is the mks permeability of free space, $4\pi\times10^{-7}$, ρ is the reciprocal of the unit-cell volume in mks units, ν_p is the phonon frequency in cm^{-1}, h is Planck's constant (mks), and c is the speed of light in cm/sec. [The mixed units are necessary in order that the mks expressions used to obtain (34) lead to integrated absorption in the normal units of cm^{-2}.] Substituting for $|\delta M_x|^2/N$, we obtain

$$\begin{aligned} \int\alpha\,d\nu &= \frac{2\pi^2 n\mu_0\rho\nu_p}{hc}\,\frac{3\mu_B^2}{(\hbar\omega_p)^2}\,\frac{\hbar}{2m\omega_p} \\ &\times\left\{\frac{\omega_0(T)^2\omega_p^2}{[\omega_p^2-\omega_0(T)^2]^2}\left[\frac{M(T)}{M(0)}\right]^2[A(T)g_x\eta+C(T)g_y\xi]^2\right. \\ &\left.+\frac{\omega_p^4}{[\omega_p^2-\omega_0(T)^2]^2}\tanh^2\left(\frac{\hbar\omega_0(T)}{2kT}\right)\right. \\ &\left.\times[A(T)g_x\xi-C(T)g_y\eta]^2\right\} . \end{aligned} \tag{36}$$

IV. RESULTS

By fitting the theory derived in Sec. III to the experimental results in Sec. II, one can extract two sets of local spin-phonon interaction parameters (η, ξ). In particular, the shape of the curve of transferred magnetic-dipole intensity versus temperature determines the relative magnitude of η and ξ and the integrated intensity at $T=0\,^\circ\mathrm{K}$ determines the absolute magnitude. We begin by enumerating the single-ion parameters used in the remaining discussion. The temperature dependence of the matrix elements, $A(T)$ and $C(T)$, produced by the exchange mixing of the Kramers doublets below the Néel point are then calculated. At this point everything in Eq. (36) except η and ξ is specified. We then extract η and ξ by fitting (36) to Fig. 2.

The single-ion parameters with which we characterize the effective $S=\frac{3}{2}$ manifold are

$$\begin{aligned} &+\delta=24\ \mathrm{cm}^{-1} , \quad \gamma=43\ \mathrm{cm}^{-1} , \\ &g_x=1.8 , \quad g_y=2.6 , \quad g_z=2.6 . \end{aligned} \tag{37}$$

These values are taken from the data on Co^{2+} in MgF_2 given by Parisot *et al.*,[37] Johnson *et al.*,[38] and by Gladney.[34,39] They do not perfectly describe the manifold. The parameters have been chosen to reproduce the energy of the excited doublet, 157 cm^{-1}, precisely and give a best fit to the observed g factors for the two doublets. A comparison between the energy and g factors predicted by these parameters and those observed is shown in Table I. The most serious discrepancy appears for g_x in the ground doublet. The 30% difference between the spin Hamiltonian g_x and the experimental g_x is not as significant as would first appear. Since $g_y^2 \gg g_x^2$, the response of the pure CoF_2 system to transverse

TABLE I. Single-ion spectroscopic parameters deduced from Co^{2+} in MgF_2 compared with predictions of spin Hamiltonian (1) with values of δ, γ, and g given by (37).

		Spin Hamiltonian	$Co^{2+}MgF_2$ (Refs. 34, 37–39)
	ϵ_0	157	$157\pm0.5\ \mathrm{cm}^{-1}$
Ground state	g_z	4.16	4.240
	g_x	1.68	2.296
	g_y	6.027	6.027
Excited state	g_z	1.26	1 ± 0.2
	g_x	5.19	5 ± 1.5
	g_y	0.89	...

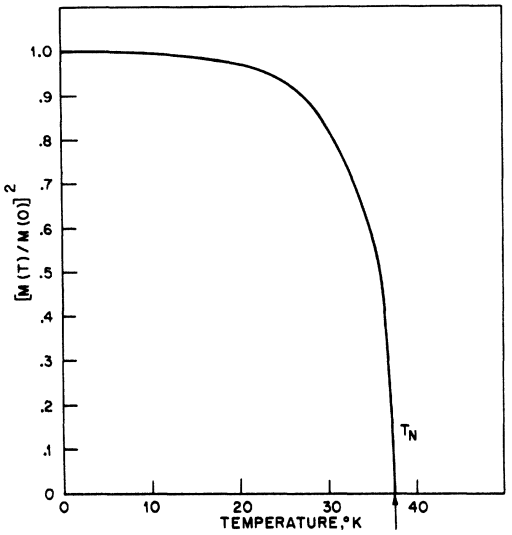

FIG. 8. Square of the sublattice magnetization versus temperature (Ref. 5).

magnetic fields is determined primarily by g_y.[40] The inaccuracies in g_x do not appear important in the final analysis.[41]

The temperature-dependent molecular field alters the matrix elements A and C as shown in (33), where $\alpha(T)$ can be written as

$$\alpha(T) = zJ \langle S \rangle_{T=0^\circ K} \frac{M(T)}{M(0)} , \tag{38}$$

where $M(T)/M(0)$ is the sublattice magnetization measured by neutron[5] diffraction and normalized to unity at $T = 0\,^\circ$K. The square of this parameter is plotted in Fig. 8. $\langle S \rangle_{T=0\,^\circ K}$ is the average spin at $T = 0\,^\circ$K taken to be 1.13, the value obtained in the second of these papers from the longitudinal-spin-wave energies. It differs from the NMR value by ~8%. Throughout this calculation we neglect exchange interactions between the body-centered ion and its two nearest neighbors. It is expected from the work of Lines[8] and from the work of Martel *et al.*[5] that

$$z_2 J_2 / z_1 J_1 \gtrsim 20 . \tag{39}$$

Neglecting $z_1 J_1$, we take $z_2 J_2$ equal to zJ equal to 31.8 cm^{-1}, determined again in the second paper from the longitudinal-spin-wave energies at $T = 0\,^\circ$K. This value differs by approximately 10% from the value given by Lines and by 5% from that given by Belorizky *et al.*[42] Using these parameters in (38) and subsequently in (33) we obtain for the temperature-dependent matrix elements $A(T)$ and $C(T)$

$$\begin{aligned} A(T) &= -0.058 - 0.20 M(T)/M(0) , \\ C(T) &= 1.00 - 0.20 M(T)/M(0) . \end{aligned} \tag{40}$$

The temperature-dependent exciton energy $\omega_0(T)$ may be taken from the neutron-diffraction results[5] or far-infrared absorption, both of which are plotted in Fig. 9. The solid line interpolates between the two sets of data and is used for $\omega_0(T)$.

Two remaining temperature-dependent factors in expression (36) must be determined. They are

$$\frac{\omega_p^4}{[\omega_p^2 - \omega_0^2(T)]^2} \tanh^2 \frac{\hbar \omega_0(T)}{2kT} \tag{41}$$

and

$$\frac{\omega_p^2 \omega_0^2(T)}{[\omega_p^2 - \omega_0(T)^2]^2} \left(\frac{M(T)}{M(0)} \right)^2 . \tag{42}$$

With $\omega_p = 245$ cm^{-1}, $\omega_0(T)$ given by Fig. 9, and $[M(T)/M(0)]^2$ shown in Fig. 8, we plot the factors (41) and (42) in Fig. 10.

Two sets of interaction constants (η, ξ) can be deduced by requiring that (36) fit the experimental intensity-versus-temperature curve in Fig. 2. They are

$$\begin{aligned} (\hbar/2m\omega_p)^{1/2} \eta &= 17.5 \text{ cm}^{-1} , \\ (\hbar/2m\omega_p)^{1/2} \xi &= 21.6 \text{ cm}^{-1} \end{aligned} \tag{43}$$

and

$$\begin{aligned} (\hbar/2m\omega_p)^{1/2} \eta &= 21.5 \text{ cm}^{-1} , \\ (\hbar/2m\omega_p)^{1/2} \xi &= -26.6 \text{ cm}^{-1} . \end{aligned} \tag{44}$$

The curves generated by these two sets of parameters are shown in Figs. 11(a) and 11(b). The experimental points are also shown for comparison. There is little to distinguish the two theoretical curves and we must accept as possible the two sets of parameters given in (43) and (44). It should be noted that we can also multiply all the parameters given in (43) and (44) by a minus sign and obtain the same result so that in fact there are four possibilities.

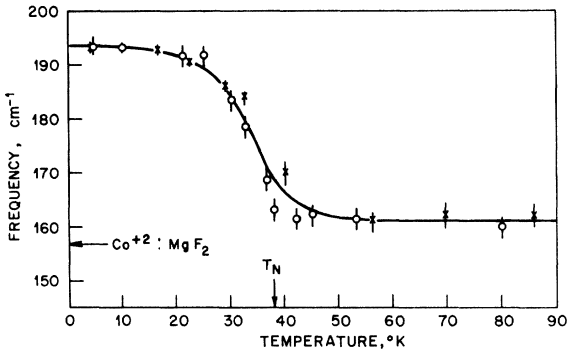

FIG. 9. Exciton frequency versus temperature: x far-infrared absorption in either α or π polarization; o inelastic neutron scattering (Ref. 5).

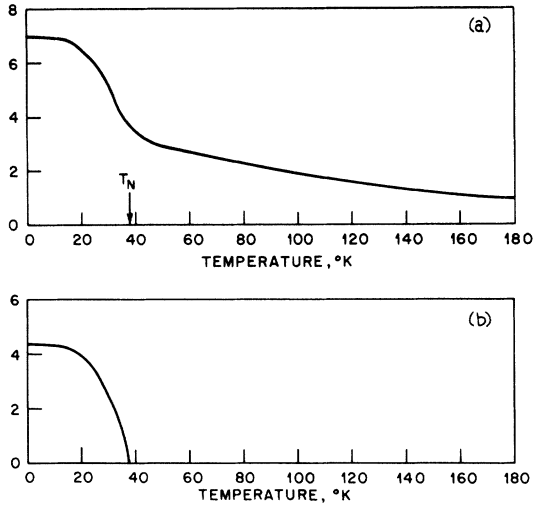

FIG. 10. (a) $\dfrac{\omega_p^4}{[\omega_p^2-\omega_0(T)^2]^2}\tanh^2\dfrac{\hbar\omega_0(T)}{2kT}$,

(b) $\dfrac{\omega_p^2\omega_0(T)^2}{[\omega_p^2-\omega_0(T)^2]^2}\left(\dfrac{M(T)}{M(O)}\right)^2$.

In Fig. 11 we also separate the two contributions to the intensity, one term proportional to the long-range-order parameter squared and the second proportional to the square of the Boltzmann weighting factor for the exciton state. In the previous discussion of this effect the entire dependence could be accounted for by the latter. In the present discussion we have included the temperature dependence of the matrix elements, thereby upsetting the agreement obtained with the second term alone. The first term, proportional to the square of the long-range-order parameter, must then be included to obtain good agreement.

V. DISCUSSION

In the preceding discussion we have shown how a detailed analysis of the temperature dependence of the magnetic-dipole intensity transferred to the E_g optical phonon from the exciton can be used to extract the local microscopic spin-lattice coupling parameters. The shape of the intensity-versus-temperature curve gives the relative strengths of the two interaction constants and the absorption strength their absolute magnitudes. That we can determine two parameters from the single curve follows from the fact that there are two distinct contributions to the transferred intensity. The first is proportional to the long-range-order parameter squared and appears only below T_N and the second is proportional to the Boltzmann distribution factor for the exciton states. The relative contributions of these two terms determine the shape of the curve. Since the strength of these two terms depends in a different manner on η and ξ we can deduce the two parameters.

At this point we would do well to enumerate the various assumptions and approximations used to obtain these results.

(a) We have assumed a strictly local spin-lattice interaction given by two constants η and ξ. If the spin interacted strongly with distortions in other unit cells clearly, we would require more parameters. However, restricting our discussion to $k=0$, the final result would again contain only two parameters which would be suitable averages over the many parameters introduced by the long-range interactions. The complexities introduced by including such possibilities hardly seem justified at this time. However, it must be noted that η and ξ may not describe a strictly local spin-lattice interaction

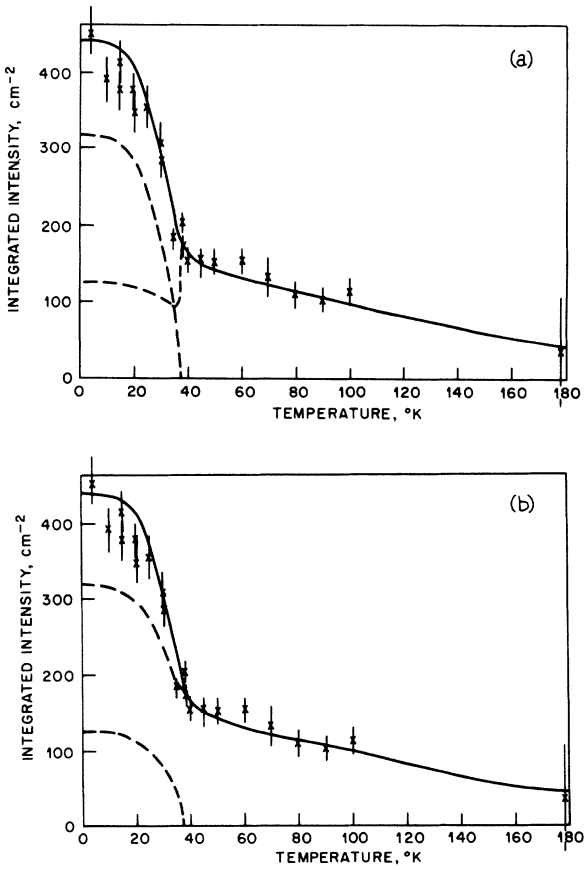

FIG. 11. Integrated intensity versus temperature.
(a) $(\hbar/2m\omega_p)^{1/2}\,\eta=21.5\ \text{cm}^{-1}$, $(\hbar/2m\omega_p)^{1/2}\,\xi=-26.6\ \text{cm}^{-1}$,
(b) $(\hbar/2m\omega_p)^{1/2}\,\eta=17.5\ \text{cm}^{-1}$, $(\hbar/2m\omega_p)^{1/2}\,\xi=21.6\ \text{cm}^{-1}$.
The dashed curves show the relative contributions made by the two terms in Eq. (36) below T_N. The experimental points are shown for comparison.

but rather an average over an extended interaction, albeit weighted most strongly in the unit cell containing the spin. The fact that we consider only interactions with the $Q_{\epsilon x}$ and $Q_{\epsilon y}$ moments does not impair the analysis as long as we consider only interactions with the E_g modes.

(b) The assumption that the low-energy single-ion properties can be obtained from the experiments on Co^{2+} in MgF_2 is probably good to within 5% or better with regard to both energies and wave functions.

(c) The description of the single-ion properties in terms of the simple spin Hamiltonian introduces further errors into the calculation. Taken with assumption (b), this probably introduces errors as large as 10–15% in the final analysis primarily due to inaccuracies in the g factors used in expression (26).

(d) We further approximate the effects of exchange mixing between the doublets by the first-order terms alone. That is, the temperature dependence of the matrix elements $A(T)$ and $C(T)$ contains terms higher than first order in $M(T)/M(0)$. There omission introduces errors of the order of 10%.

(e) Lastly we have treated the spin system in the molecular field approximation. This is a reasonable assumption since the spin excitations that interact with the E_g phonons have no significant dispersion either above or below the transition temperature. Neglect of J_1 and higher-order spin interactions introduces errors of the order of 5%. Taken as a whole these assumptions and approximations lead to uncertainties of the order of ~30% in the determination of η and ξ.

It may be noted that the order of magnitude of the interaction parameters agrees with some estimates we may make. The orbital states in the d^7 configuration are split by ~10 000 cm^{-1} by a *unit* strain. The phonon motion generates a strain of approximately 0.02 which will give an interaction then of 200 cm^{-1}. However, the orbit-lattice interaction produces a spin-lattice interaction by virtue of the spin-orbit coupling ($\lambda \sim 230$ cm^{-1}) with the excited states at $\Delta E \sim 1000$ cm^{-1}. This gives a spin-phonon interaction $(\lambda/\Delta E)^2$ times the orbit-phonon interaction, resulting in a spin-phonon coupling of ~12 cm^{-1}. This is of the same order of magnitude as obtained for $(\hbar/2m\omega_p)^{1/2}\eta$ and $(\hbar/2m\omega_p)^{1/2}\xi$ in (43) and (44).

In the paper that follows we examine more closely the spin-wave excitations. In particular, we show how a good quantitative description of all the low-lying $k = 0$ spin excitations can be obtained by including the phonon interaction obtained above, in an otherwise simple description of the spin excitations.

ACKNOWLEDGMENTS

The authors would like to thank P. Martel for providing an additional sample of CoF_2. They have also benefitted from discussions with L. R. Walker and M. E. Lines and wish to thank R. G. MacFarlane, S. Ushioda, and D. L. Mills for communicating their results prior to publication. The technical assistance of F. DeRosa is gratefully acknowledged.

[1]R. A. Erickson, Phys. Rev. 90, 779 (1953).

[2]T. Nakamura and H. Taketa, Progr. Theoret. Phys. (Kyoto) 13, 129 (1955).

[3]J. W. Stout and L. M. Matarrese, Rev. Mod. Phys. 25, 338 (1953).

[4]P. L. Richards, J. Appl. Phys. 35, 850 (1964).

[5]R. A. Cowley, P. Martel, and R. W. H. Stevenson, Phys. Rev. Letters 18, 162 (1967); P. Martel, R. A. Cowley, and R. W. H. Stevenson, Can. J. Phys. 46, 1355 (1968).

[6]A. S. Barker, Jr. and J. A. Ditzenberger, Solid State Commun. 3, 131 (1965).

[7]H. Kamimura, J. Appl. Phys. 35, 844 (1964).

[8]M. E. Lines, Phys. Rev. 137, A982 (1965).

[9]J. H. Van Vleck, J. Phys. Radium 12, 262 (1951).

[10]K. W. H. Stevens, Rev. Mod. Phys. 25, 166 (1953).

[11]T. Moriya and K. Yosida, Progr. Theoret. Phys. (Kyoto) 9, 663 (1953).

[12]P. M. Levy, Phys. Rev. Letters 20, 1366 (1968); Phys. Rev. 147, 311 (1966); 135, A155 (1964).

[13]R. J. Elliot and M. F. Thorpe, J. Appl. Phys. 39, 802 (1968).

[14]R. J. Birgeneau, M. T. Hutchings, J. M. Baker, and J. D. Riley, J. Appl. Phys. 40, 1070 (1969), and references contained therein.

[15]T. Moriya, Phys. Rev. 120, 91 (1960).

[16]I. Dzialoshinski, J. Phys. Chem. Solids 4, 241 (1958).

[17]R. Orbach and M. Tachiki, Phys. Rev. 158, 524 (1967).

[18]J. M. Baker and A. F. Mau, Can. J. Phys. 45, 403 (1967).

[19]D. H. McMahon and R. H. Silsbee, Phys. Rev. 135, A91 (1964).

[20]S. J. Allen, Jr., Phys. Rev. 166, 530 (1968).

[21]S. J. Allen, Jr., Phys. Rev. 167, 492 (1968).

[22]K. A. Hay and J. B. Torrance, Jr., J. Appl. Phys. 40, 999 (1969).

[23]G. Dolling and R. A. Cowley, Phys. Rev. Letters 16, 683 (1966).

[24]T. Moriya, J. Phys. Chem. Solids 11, 73 (1959).

[25]A. S. Borovik-Romanov, Zh. Eksperim. i Teor. Fiz. 36, 1954 (1959) [Sov. Phys. JETP 9, 1390 (1959)].

[26]P. L. Richards (unpublished).

[27]B. Golding (unpublished).

[28]G. A. Slack, Phys. Rev. 122, 1451 (1961).

[29]S. J. Allen, Jr. and H. J. Guggenheim, Phys. Rev. Letters 21, 1807 (1968).

[30]D. L. Mills and S. Usihoda, Phys. Rev. B 2, 3815 (1970). Recently Mills and Ushioda have constructed a theory of the anomalous dependence of linewidth on temperature. Essential to the theory is either little or no temperature dependence of the linewidth of the electronic

state below T_N (as might be inferred from the neutron data[5]). The far-infrared data, which suffer less from instrumental limits on the resolution, indicate, however, a rather dramatic increase in linewidth which dominates the results of the theory and produces the opposite effect—a line broadening at the Néel point. Although the basic idea proposed by Mills and Ushioda may be correct, in its present form it does not appear to properly describe the experimental results.

[31]P. L. Richards, J. Opt. Soc. Am. 54, 1474 (1964).

[32]R. M. MacFarlane and S. Ushioda, Solid State Commun. 8, 1081 (1970); R. M. MacFarlane, Phys. Rev. Letters 25, 1454 (1970).

[33]S. P. S. Porto, P. A. Fleury, and T. C. Damen, Phys. Rev. 154, 522 (1967).

[34]H. M. Gladney, Phys. Rev. 146, 253 (1966).

[35]P. S. Narayanan, Proc. Indian Acad. Sci. 32A, 279 (1950).

[36]J. M. Ziman, *Electrons and Phonons* (Oxford U. P., London, 1960), p. 16f.

[37]G. Parisot, S. J. Allen, Jr., R. E. Dietz, H. J. Guggenheim, R. Moyal, P. Moch, and C. Dugautier, J. Appl. Phys. 41, 890 (1970).

[38]L. F. Johnson, R. E. Dietz, and H. J. Guggenheim, Appl. Phys. Letters 5, 21 (1964).

[39]H. M. Gladney, Phys. Rev. 143, 198 (1966).

[40]This is true for magnetic fields in either the x or y direction. It must be noted that the two sites in CoF_2 differ by a rotation of 90°. Consequently, when a field is applied in the x direction, the magnetization on the site in question is proportional to g_x^2 but the magnetization on the opposite side will be proportional to g_y^2.

[41]We have tacitly assumed that the spin-phonon coupling in Co^{2+}, MgF_2 does not significantly perturb the 157-cm^{-1} splitting. Since the energy separation of this state and the E_g phonon is five times larger in MgF_2 than in CoF_2, we expect that it may perturb the excited doublet of Co^{2+} in MgF_2 by no more than ~ 3 cm^{-1} ($\sim 2\%$). We choose to ignore such a correction.

[42]E. Belorizky, S. C. Ng, and T. G. Phillips, Phys. Rev. 181, 467 (1969).

PHYSICAL REVIEW B VOLUME 4, NUMBER 3 1 AUGUST 1971

Magnetic Excitations in Antiferromagnetic CoF_2. II. Uniform Magnetic Excitations near $T = 0$ °K

S. J. Allen, Jr. and H. J. Guggenheim
Bell Telephone Laboratories, Murray Hill, New Jersey 07974

(Received 11 January 1971)

Far-infrared absorption experiments on CoF_2 at 4.2 °K are extended to include all the uniform magnetic excitations below 300 cm^{-1}. The linear and nonlinear Zeeman effect, obtained with externally applied magnetic fields parallel and perpendicular to the spin direction, are also observed. A model of the uniform magnetic excitations derived from an effective $S = \frac{3}{2}$, Co^{2+} manifold is constructed by including a large orthorhombic anisotropy field, determined from Co^{2+} in MgF_2, a simple isotropic bilinear exchange, and the independently determined spin-phonon coupling to the E_g optical phonon. The model gives a satisfactory account of the energies, linear and nonlinear Zeeman effect, as well as the absorption intensities.

I. INTRODUCTION

In the preceding paper the coupling between the Co^{2+} effective $S = \frac{3}{2}$ spin and the E_g optical phonon was discussed at length—the object being to extract from the temperature dependence of transferred magnetic-dipole intensity some microscopic parameters describing the spin-lattice interaction. In the present discussion, we focus our attention on the spin system and attempt to derive a quantitative description of the uniform, $k = 0$, magnetic excitations at $T = 0$ °K that evolve from the effective $S = \frac{3}{2}$ manifold. Experimentally we have extended the far-infrared absorption experiments of Barker and Ditzenberger[1] as well as Richards[2] to include all the uniform magnetic excitations of the system at 4.2 °K below 300 cm^{-1}. The Zeeman effect both parallel and perpendicular to the spin axis is obtained. The work confirms the $k = 0$ excitation energies obtained by neutron diffraction[3] and agrees with recent Raman scattering experiments by MacFarlane.[4]

The spectrum of excitations that evolve from the Co^{2+} ion when it is found in a concentrated salt such as CoF_2 may be viewed from two points of view. In the first case one may consider all but the lowest excitation to be excitons, perturbed to a greater or lesser extent by the Co^{2+}-Co^{2+} interactions, while the lowest excitation is a spin wave. It is distinguished from the excitons only by the fact that in the absence of Co^{2+}-Co^{2+} interactions the spin waves have zero excitation energy while the excitons retain a finite energy. With reference to Fig. 1, for instance, the 12 levels derived from the $^4\Gamma_4$ in the ordered state will contribute eleven single-particle-like excitations to the collective